ENTROPY COORDINATE, QUASI-GEOSTROPHIC TURBULENCE AND THE DESIGN OF LATERAL DIFFUSION IN GENERAL CIRCULATION MODELS.

Robert Sadourny
Laboratoire de Météorologie Dynamique
Paris, France

1. INTRODUCTION

Among the various subgrid scale parameterisations which must be included in general circulation models, lateral diffusion concerns the relatively well defined problem of how the resolved scales are affected by the sub-grid scales in the nonlinear processes of "horizontal" dynamics. Horizontal dynamics, however, is a rather vague term, and should be preferably replaced by "isentropic" dynamics, or "quasi-geostrophic" dynamics, which both have a coherent dynamical meaning. Of the two definitions, the latter is easiest to use, because we can then rely on quasi-geostrophic turbulence theories to formulate lateral diffusion schemes. On the other hand, it is only an approximation, and we must eventually go back to formulating lateral diffusion schemes in the primitive equation framework : for this particular step, the isentropic formulation is most convenient, because it is, as we shall show, particularly close to the quasi-geostrophic equations.

We shall then proceed as follows. In section 2, we shall try to clarify isentropic dynamics and its relation to quasi-geostrophic dynamics ; in section 3, we shall expand on the phenomenological theory of barotropic quasi-geostrophic turbulence and its implications for lateral diffusion schemes ; in section 4, we shall address the baroclinic problem in a similar way. In the course of our derivations, we shall try to reach better understanding of the importance of lateral diffusion design : in particular we shall demonstrate its crucial importance in low resolution general circulation or quasi-geostrophic models, when it interferes with baroclinic instability processes. The problem addressed here therefore concerns mainly climate- and long-range forecasting models, for which explicit resolution of unpredictable transients is not a priori the best choice.

2. BASIC EQUATIONS

2.1. General form of the primitive equations in entropy coordinate.

If we neglect the effect of moisture, the equation of state can be written in the general form

$$h = H\ (s,p), \tag{1}$$

where h is enthalpy, p pressure and s any function of entropy ; here the perfect gas assumption has not necessarily been made. An equivalent form is

$$\alpha = H_p\ (s,p), \tag{2}$$

where α is specific volume and the index p refers to partial derivation with respect to p at constant s .

In the hydrostatic case, for any vertical coordinate system, the horizontal equation of motion may be written

$$\frac{D\underline{V}}{Dt} + f\ \underline{N} \times \underline{V} + \text{grad}\ \phi + \alpha\ \text{grad}\ p = 0\ . \tag{3}$$

This holds because the hydrostatic geopotential-pressure force is horizontal and therefore can be evaluated along any sloping surface.

The use of entropy as vertical coordinate yields some remarkable simplifications of the primitive equations. Firstly, s is a lagrangian coordinate, since in the absence of heat sources

$$\dot{s} \equiv Ds/Dt = 0\ ; \tag{4}$$

therefore all vertical advection terms disappear. Secondly, from (2 , 3), the geopotential and pressure gradients can be lumped together in the horizontal equation of motion, which reads

$$\frac{D\underline{V}}{Dt} + f\ \underline{N} \times \underline{V} + \text{grad}\ S = 0\ ; \tag{5}$$

The dry static energy

$$S = \phi + h \tag{6}$$

is sometimes named "Montgomery potential". The continuity equation is readily written in terms of a "pseudo-density"

$$r = - \partial p/\partial s \tag{7}$$

which must be always positive ; it reads

$$\frac{\partial r}{\partial t} + \text{div } (r\underline{V}) = 0 \tag{8}$$

(in this section div, grad and curl refer to horizontal derivation operators). A further advantage of the entropy coordinate formulation is the very simple form of (hydrostatic) Ertel's potential vorticity equation :

$$D\eta/Dt = 0 \tag{9}$$

which is readily obtained from (5 , 8) and the definition

$$\eta = (f + \text{curl } V)/r. \tag{10}$$

The rigid lower boundary must be prescribed as a moving boundary in the s-coordinate frame of reference : $s_B\ (x,y,t)$; it moves according to

$$Ds_B/Dt = 0 \tag{11}$$

in the absence of heat sources. Rigidity is expressed by imposing a prescribed surface geopotential $\phi_B\ (x,y)$:

$$\phi\ (x,y,s_B\ (x,y,t),t) = \phi_B\ (x,y). \tag{12}$$

At the top we usually impose a free upper boundary with constant pressure $\bar{p}_T$. The top boundary is defined by the surface $s = s_T(x,y,t)$, which moves according to

$$Ds_T/Dt = 0 \qquad (13)$$

again in the absence of heat sources, and over which we impose

$$p(x,y,s_T(x,y,t),t) = \bar{p}_T. \qquad (14)$$

Note that the governing equations in the inside of the fluid (5 , 8) are two-dimensional equations formally similar to Saint-Venant's shallow water equations — except that in the latter, S and r reduce to a single dependent variable. Here r is a prognostic variable, and S is diagnostically obtained by solving a one-dimensional (vertical) nonlinear elliptic problem, expressed by boundary conditions (11, 14), and, in-between, the hydrostatic equation,

$$\partial S/\partial s = H_s(s,p). \qquad (15)$$

The free surface boundary condition at the top (14) appears as a boundary condition of Neuman type, while the rigid condition at the bottom (12) is of mixed Dirichlet-Neuman type.

For a perfect gas, and the definition $s = c_p T p^{-\kappa}$, this vertical coupling problem reduces to the very simple form

$$\begin{aligned} &\frac{\partial S}{\partial s} = p_T^{\kappa} && \text{at} \quad s = s_T\,, \\ &-\frac{\partial}{\partial s}\left(\frac{\partial S}{\partial s}\right)^{1/\kappa} = r && \text{for} \quad s_B < s < s_T\,, \\ &\left(1 - s\,\frac{\partial}{\partial s}\right) S = \phi_B && \text{at} \quad s = s_B\,. \end{aligned} \qquad (16)$$

The invariants of the problem are : the energy E

$$E = \iint_D \left(p_B \phi_B + \int_{s_B}^{s_T} \left(\frac{V^2}{2} + h\right) r\,ds \right) dxdy , \qquad (17)$$

and the vertical distribution of any function of potential vorticity :

$$P_A(s) = \iint_{D'(s,t)} A(\eta,s)\, r\, dxdy. \qquad (18)$$

Here D is the spherical domain and

$$D'(s,t) = D \cap \{(x,y) \,|\, s_B(x,y,t) < s < s_T(x,y,t)\}.$$

The most useful choice for (18) is the vertical distribution of potential enstrophy

$$P(s) = \iint_{D'(s,t)} \frac{\eta^2}{2}\, r\, dxdy. \qquad (19)$$

Note that if the derivation of (18, 19) is straightforward from (8,9,11,13), the derivation of (17) is on the contrary, rather delicate from (5,8,11-15) ; it requires scalar multiplication of (5) by $r\underline{V}$, multiplication of (8) by S, adding the two and finally integrating by parts with meticulous treatment of moving boundaries.

——————— p, H_s

..... $\underline{V}$,r,S

——————— p, H_s

..... $\underline{V}$,r,S

Figure 1.

It follows from what has just been said that the simplest finite difference models of (5,8,15) based on figure 1, are energetically consistent ; at the same time, they keep accurate track of Ertel's potential vorticity dynamics. The fact that these two properties are simultaneously obeyed is another attractive aspect of entropy coordinate models (for a general discussion of this topic, see Arakawa, 1984).

2.2. Entropy coordinate and the quasi-geostrophic approximation

The derivation of the quasi-geostrophic approximation is particularly straightforward

in entropy coordinate because of its Lagrangian character, associated with the simple form of Ertel's potential vorticity theorem.

Splitting all variables into sums of mean and perturbation values, viz : $f = \bar{f} + f'$, $p = \bar{p}(s) + p'$, then $\bar{r} = -\, d\bar{p}/ds$, $\bar{h} = H(s,\bar{p})$ etc ..., the assumptions

$$
\begin{aligned}
& f' \,/\, \bar{f} = O(\varepsilon), \\
& w' \,/\, \bar{f} = O(\varepsilon), \\
& \mu' \,/\, \bar{f} = O(\varepsilon) \qquad \text{or Ro} = O(\varepsilon) \quad , \\
& r' \,/\, \bar{r} = O(\varepsilon) \qquad \text{or } (\text{RoRi})^{-1} = O(\varepsilon),
\end{aligned}
\tag{20}
$$

where w' refer to linear eigenfrequencies and μ' to nonlinear advective characteristic frequencies, yield to first order in the small parameter ε, the quasi-geostrophic approximation :

$$
\underline{V} = \underline{N} \times \text{grad } \Psi \;, \qquad \Psi = S'/\bar{f} \;, \tag{21}
$$

and

$$
\frac{Dq}{Dt} = 0 \quad , \qquad q = f + \mathfrak{D}\Psi, \tag{22}
$$

with the definition

$$
\mathfrak{D} = \nabla^2 + \frac{\bar{f}^2}{\bar{r}} \frac{\partial}{\partial s} \left(\frac{\partial}{\partial s} \,/\, \bar{\alpha}_s \right) \tag{23}
$$

The quasi-geostrophic potential vorticity q is just a first order expansion of Ertel's potential vorticity η, (22,23) being a straightforward expansion of (9,10). Note that the vertical laplacian in (23) is just a linearization of the nonlinear laplacian already mentioned for the primitive equations.

The quantity q is often refered to as a pseudo-potential vorticity, because it appears from the more classical derivations in z or p coordinate, as a pseudo-invariant conserved only in the horizontal projection of the motion (e.g : Charney and Flierl, 1981). It appears from the present derivation however, that q is

actually a true lagrangian invariant of the full quasi-geostrophic motion ; this is another advantage of the entropy coordinate framework.

Boundary conditions (11-14) on the fluctuating surfaces $\bar{s}_B = \bar{\bar{s}}_B + s'_B(x,y,t)$, $s_T = \bar{\bar{s}}_T + s'_T(x,y,t)$, are not directly usable in the quasi-geostrophic approximation. They have to be approximated on flat surfaces $s_B = \bar{\bar{s}}_B$, $s_T = \bar{\bar{s}}_T$, using the assumptions

$$\frac{s'_T}{p}\frac{\partial p}{\partial s} = O(\varepsilon) \qquad \text{at} \quad s = \bar{\bar{s}}_T \ , \tag{24}$$

$$\frac{s'_B}{\phi}\frac{\partial \phi}{\partial s} = O(\varepsilon) \qquad \text{at} \quad s = \bar{\bar{s}}_B .$$

Then the quasi-geostrophic boundary conditions read

$$\frac{Dp'}{Dt} = 0 \qquad \text{at } s = \bar{\bar{s}}_T \ , \tag{25}$$

$$\frac{D}{Dt}(\phi' - \phi'_B) = 0 \qquad \text{at } s = \bar{\bar{s}}_B \ , \tag{26}$$

where ϕ'_B is defined by $\phi_B(x,y) = \bar{\phi}_B + \phi'_B(x,y)$, and the pressure and geopotential perturbations are obtained by

$$p' = \bar{\bar{f}}\frac{\partial \Psi}{\partial s} / \bar{\alpha}_s \ , \tag{27}$$

$$\phi' = \bar{\bar{f}}\left(1 - \bar{\alpha}/\bar{\alpha}_s \frac{\partial}{\partial s}\right)\Psi . \tag{28}$$

The invariants (17-19) of the primitive equations have straightforward equivalents in the quasi-geostrophic system :

$$E = \frac{1}{2}\iint_D dxdy\left\{\bar{\bar{f}}^2 \Psi^2 / \bar{\alpha}\Big|_{s=\bar{\bar{s}}_B} + \int_{\bar{\bar{s}}_B}^{\bar{\bar{s}}_T} ds\left(\bar{r}\,(\mathrm{grad}\Psi)^2 + \frac{\bar{\bar{f}}^2}{\bar{\alpha}_s}\left(\frac{\partial \Psi}{\partial s}\right)^2\right)\right\} \tag{29}$$

$$P_A(s) = \iint_D A(q,s)\, dxdy \ , \tag{30}$$

$$P(s) = \iint_D \frac{q^2}{2}\, dxdy \ , \tag{31}$$

respectively, the energy and the (generalized or quadratic) potential enstrophy. The quasi-geostrophic system has however, two supplementary invariants :

$$P_A\ (\bar{s}_T) = \iint_D A(p')\, dxdy \ , \tag{32}$$

$$P\ (\bar{s}_T) = \iint_D \frac{p'^2}{2}\, dxdy \ , \tag{33}$$

$$P_A(\bar{s}_B) = \iint_D A\ (\phi' - \phi'_B)\ \ dxdy \ , \tag{34}$$

$$P\ (\bar{s}_B) = \iint_D \frac{1}{2}\ (\phi' - \phi'_B)^2\ dxdy \ , \tag{35}$$

respectively the (generalized or quadratic) available potential energies on top and bottom boundaries. All these invariants are, however, approximately conserved by the primitive equations as soon as assumptions (24) — small fluctuations of upper and lower boundaries around isentropic surfaces — are made.

Coming now to the problem of lateral diffusion, one again finds a definite advantage is using entropy as vertical coordinate, because of the simplified formulation of Ertel's potential vorticity dynamics. In fact, lateral diffusion can be designed using the simple framework of quasi-geostrophic dynamics ; its extension to the primitive equation case is then straightforward if the entropy coordinate is used, because of the similarity between Ertel's equation and the quasi-geostrophic vorticity equation. The simplest case of barotropic flow is considered in section 3 ; section 4 deals with the general baroclinic case.

3. QUASI-GEOSTROPHIC TURBULENCE AND LATERAL DIFFUSION : THE BAROTROPIC CASE

3.1. The barotropic equations

Strictly speaking, barotropicity is the supplementary constraint that all thermodynamic variables are functions of s only. Adding this constraint to the primitive equations yields div $\underline{V} = 0$, because $r = \bar{r}(s)$ in the continuity equation (8) ; thus, barotropic flow is horizontally non divergent. Furthermore, grad S, because of (15) becomes independent of s ; then $\underline{V}$ must also be independent of s if the equation of motion (5) is to be satisfied. Thus barotropic flow is governed by the two-dimensional Euler equation

$$\frac{Dq}{Dt} = 0 \quad (\text{with } q = f + \nabla^2 \psi,\ \underline{V} = \underline{N} \times \text{grad}\Psi). \tag{36}$$

and therefore, cannot react to bottom orography.

A less restrictive approach is to start from the general quasi-geostrophic model (21-23, 25-28), and assume that $\underline{V}$ departs only slightly from its vertical average

$$\tilde{\underline{V}} = \underline{N} \times \text{grad}\tilde{\Psi}, \tag{37}$$

$$\tilde{\Psi} = \frac{1}{\bar{p}(\bar{s}_B) - \bar{p}_T} \int_{\bar{s}_B}^{\bar{s}_T} \Psi \, \bar{r} \, ds. \tag{38}$$

Then, to first order, D/Dt becomes independent of s and (22) can be integrated vertically to yield, after use of boundary conditions (25-28) :

$$\frac{D\tilde{q}}{Dt} = 0 , \quad \tilde{q} = f + (\nabla^2 - \ell_o^2)\tilde{\Psi} + \tilde{q}_B \tag{39}$$

where ℓ_o^{-1} is the external radius of deformation

$$\ell_o^2 = \bar{f}^2 \Big/ \left[\bar{\alpha}(\bar{s}_B) \left(\bar{p}(\bar{s}_B) - \bar{p}_T \right) \right] \tag{40}$$

and $\tilde{\tilde{q}}_B$ is the normalized orography

$$\tilde{\tilde{q}}_B = \bar{f}\ \phi'_B \ / \left[\bar{\alpha}\ (\bar{s}_B)\left(\bar{p}\ (\bar{s}_B) - \bar{p}_T\right)\right] \tag{41}$$

Equation (39) may be called the quasi-barotropic, quasi-geostrophic potential vorticity equation. Most parts of the discussion which follows concentrate on the dynamics of the simplified equation

$$\frac{D\tilde{q}}{Dt} = 0\ , \quad \tilde{q} = (\nabla^2 - \ell_o^2)\tilde{\Psi}\ , \tag{42}$$

in the absence of inertial or topographic Rossby waves. As usual the invariants are : total energy

$$E = \frac{1}{2}\iint_D (\mathrm{grad}\tilde{\Psi})^2 + \ell_o^2\tilde{\Psi}^2\ \mathrm{dxdy}\ , \tag{43}$$

and (generalized or quadratic) potential enstrophy

$$P_A = \iint_D A(\tilde{q})\ \mathrm{dxdy}\ , \tag{44}$$

$$P = \frac{1}{2}\iint_D \tilde{q}^2\ \mathrm{dxdy}. \tag{45}$$

Expansion of $\tilde{\Psi}$, $\tilde{q}$ in terms of real Laplacian eigenfunctions

$$\begin{aligned} \tilde{\Psi} &= \Sigma\ \tilde{\Psi}_n\ \Lambda_n\ , \\ \tilde{q} &= \Sigma\ \tilde{q}_n\ \Lambda_n\ , \\ \nabla^2\Lambda_n &= -\ k_n^2\ \Lambda_n \end{aligned} \tag{46}$$

yield the energy and quadratic potential enstrophy expansions

$$E = \Sigma\, E_n\ ,\quad E_n = -\frac{1}{2}\,\tilde{\psi}_n\tilde{q}_n$$
$$P = \Sigma\, P_n\ ,\quad P_n = \frac{1}{2}\,\tilde{q}_n^2 \qquad (47)$$

with the relation

$$P_n = (k_n^2 + \ell_o^2)\, E_n\ . \qquad (48)$$

The phenomenology of barotropic turbulence is mainly based on the invariance of E and P in nonlinear interactions. How these invariants affect the energy spectrum depends of course crucially on relation (48).

3.2. Phenomenology of fully-developed forced barotropic turbulence

Let us consider now the somewhat idealized problem of a homogeneous, isotropic turbulence on an infinite plane, forced at a given wavenumber k_I with a stationary energy injection rate ε ; from (48), this also means a stationary potential enstrophy injection rate $\pi = (k_I^2 + \ell_o^2)\varepsilon$. We assume that, for any given wavenumbers k_-, k_+ $(0 < \underline{k} < k_I < k_+ < \infty)$, we can integrate long enough to get a statistically stationary flow in the spectral range $(k_-\ ,\ k_+)$. We shall then establish the phenomenology in the "fully-developed" limit $k_- \to 0$, $k_+ \to \infty$.

We denote by ε_+ , π_+ the spectral energy and potential enstrophy fluxes towards wavenumbers greater than k_+, by ε_-, π_- the spectral energy and enstrophy fluxes towards wavenumbers smaller than k_-. The stationarity hypothesis yields

$$\varepsilon_+ + \varepsilon_- = \varepsilon, \qquad (49)$$
$$\pi_+ + \pi_- = \pi.$$

On the other hand, (48) yields

$$\pi_+ \geq (k_+^2 + \ell_o^2)\ \varepsilon_+\ , \qquad (50)$$

or, with the help of (49)

$$\pi \geq (k_+^2 + \ell_o^2)\ \varepsilon_+ .$$

In the fully-developed limit, ε_+ must tend to zero, because of the finite potential enstrophy injection rate ; then, from (49) ε_- must tend to ε. This is the well-known reverse energy cascade : in the fully-developed limit, all the energy injected must cascade towards larger and larger scales.

Applying now (48) to the wavenumber range $0 \leq k \leq k_-$, we get

$$\ell_o^2\ \varepsilon_- \leq \pi_- \leq (k_-^2 + \ell_o^2)\ \varepsilon_- , \tag{51}$$

which yields in the fully-developed limit

$$\pi_- \to \ell_o^2 \varepsilon , \quad \varepsilon_- \to \varepsilon. \tag{52}$$

This means that, at the other end of the spectrum

$$\pi_+ \to k_I^2\ \varepsilon, \quad \varepsilon_+ \to 0. \tag{53}$$

(52,53) is a slight generalization of the classical two-dimensional turbulence theory to a flow which possesses an external radius of deformation : (53) characterizes the potential enstrophy inertial range ($k > k_I$) where potential enstrophy cascades from injection scale to smaller and smaller scales at a constant rate $k_I^2\varepsilon$ in the fully developed limit ; (52) characterizes the energy inertial range ($k < k_I$) where energy cascades from injection scale to larger and larger scales at a constant rate ε. Energy is not allowed to cascade towards small scales, but a portion $\ell_o^2\varepsilon$ of the potential enstrophy injected does follow energy in its reverse cascade.

The classical phenomenology of two dimensional turbulence has been derived by Kraichnan (1967, 1971) in the slightly restrictive case $\ell_o = 0$. To get a closer look at the inertial ranges we need a phenomenological estimate of the characteristic time scale $\tau(k)$ associated with nonlinear interactions. Now, turbulence occurs because a particular structure gets distorted or strained by velocity gradients arising from the existence of larger structures. This leads us to the estimate

$$\tau(k) \sim \left(\int_0^k \frac{p^4}{p^2 + \ell_o^2} E(p)\, dp \right)^{-1/2} . \qquad (54)$$

In (54), E(p) is the one-dimensional spectral energy density :

$$E = \int_0^\infty E(p)\, dp , \qquad (55)$$

the integral being a measure of the kinetic enstrophy (a quadratic measure of velocity gradients) lying in scales larger than k^{-1}. Now, the energy and potential enstrophy cascade rates can be estimated as

$$\varepsilon_- = k\, E(k) \,/\, \tau(k) \qquad (k \leq k_I) , \qquad (56)$$

$$\pi_+ = k^3\, E(k) \,/\, \tau(k) \qquad (k \geq k_I) , \qquad (57)$$

and it remains to eliminate $\tau(k)$ between (54,56) or between (54,57) to get the energy spectrum E(k) in each inertial range. In the potential enstrophy inertial range, the result is

$$E(k) = C_+ (k_I^2 \varepsilon)^{2/3} k^{-3} \left(\mathrm{Ln} \frac{k}{k_I}\right)^{-1/3} , \qquad (58)$$

and in the energy inertial range

$$E(k) = C_- \varepsilon^{2/3} \ell_o^{-2/3} k^{-1} \left(\frac{k^2}{\ell_o^2} - \mathrm{Ln}\, (1 + \frac{k^2}{\ell_o^2}) \right)^{-1/3} . \qquad (59)$$

(58) is equivalent to Kraichnan (1971)'s classical form with logarithmic correction in the enstrophy inertial range of two-dimensional turbulence ; for $\ell_o = 0$, (59) reduces to the classical energy inertial range spectrum. If $\ell_o \ll k_I$, (59) can be approximated by

$$E(k) \sim C_- \varepsilon^{2/3} k^{-5/3} \qquad (\ell_o \ll k < k_I) , \qquad (60)$$

$$E(k) \sim 2^{1/3} C_- \varepsilon^{2/3} \ell_o^{2/3} k^{-7/3} \qquad (k \ll \ell_o). \qquad (61)$$

If $\ell_o > k_I$ the intermediate range (60) disappears. Thus the effect of an external radius of deformation is to steepen the spectrum in the energy inertial range.

Going back to the estimate (54) of $\tau(k)$ and replacing $E(p)$ by its expression (58) in the potential enstrophy inertial range, we observe that the integrand is dominated by scales much larger than k. This means that the structures which are most efficient at straining a given scale are those whose scale is much larger (in fact, close to the injection scale). This property is expressed by saying that, in the potential enstrophy inertial range, nonlinear interactions are "nonlocal" in wavenumber space. It is readily verified from (59,54) that the reverse is true within the energy inertial range. The final estimates for $\tau(k)$ using (58,60,61) are as follows

$$\tau_+ (k) \sim (\mathrm{Ln}\, \frac{k}{k_I})^{-1/3} \qquad (k > k_I)\ , \tag{62}$$

$$\tau_- (k) \sim \begin{cases} k^{-2/3} & (\ell_o \ll k < k_I)\ , \quad (63) \\ \ell_o^{2/3}\, k^{-4/3} & (k \ll \ell_o,\ k < k_I). \quad (64) \end{cases}$$

Another effect of the radius of deformation is therefore to slow down nonlinear interactions at larger scales.

The time it takes for a structure at wavenumber k_1 to significantly affect (or be affected by) another structure at wavenumber $k_2 > k_1$ can be phenomenologically estimated as

$$\tau\ (k_I,\ k_2) = \int_{k_1}^{k_2} \tau(k)\ dk. \tag{65}$$

In particular, the quantity $\tau(k,\infty)$ can be interpreted either as a regularity time (the time it takes for structures initially confined at wavenumbers $\leq k$ to excite infinitesimal scales) — or a predictability time (the time it takes for perturbations initially confined at infinitesimal scales to significantly perturb wavenumber k). It follows from (62,65) that $\tau(k,\infty)$ diverges for barotropic turbulence. Barotropic quasi-geostrophic turbulence therefore appears as regular and indefinitely predictable from simple phenomenological arguments. The fact that mathematical analysis indeed confirms the regularity property (e.g. Kato, 1967) is a strong argument in favour of the phenomenological approach.

3.3. Truncated inviscid model flows : statistical equilibria.

In numerical models, excitation cannot propagate into the sub-grid scales : therefore, the potential enstrophy cascade is blocked at the cut-off wavenumber, and the flow tends to become organised in a quite different way.

Let us consider a strictly inviscid model with N degrees of freedom, and assume that this model is a spectral model or a finite-difference model of Arakawa (1966)'s type, which therefore conserves energy and potential enstrophy exactly. Then, the image $M = \{x_n\}$,

$$x_n = (k_n^2 + \ell_o^2)^{1/2} \tilde{\psi}_n \ ,$$

of a particular solution in the N-dimensional phase space, remains on the intersection C of the energy hypersphere

$$\sum_{n=1}^{N} x_n^2 = E \ ,$$

and the potential enstrophy hyperellipsoid

$$\sum_{n=1}^{N} (k_n^2 + \ell_o^2) x_n^2 = P \ .$$

We now demonstrate that the motion of $\underline{M}$ is nondivergent in phase space. The spectral transform of the potential vorticity equation (39) reads

$$\frac{dx_n}{dt} = \sum_{\substack{n'=1 \\ n''=1}}^{N} A_{n\,n'n''}\, x_{n'}\, x_{n''} \ . \tag{66}$$

An eigenfunction A_n is a stationary solution of (39) ; therefore

$$A_{n'n\,n} = 0. \tag{67}$$

On the other hand, the "triadic" forms of energy- and potential enstrophy conservation read

$$(k_n^2 + \ell_o^2)\, A_{n\,n'n''} + (k_{n'}^2 + \ell_o^2)\, A_{n'n''n} + (k_{n''}^2 + \ell_o^2)\, A_{n''n\,n'} = 0 \ , \tag{68}$$

$$A_n + A_{n'} + A_{n''} = 0 \ .$$

From (67,68) we have

$$A_{n\,n'n} = A_{n\,nn'} = 0 \ ,$$

or in other words

$$\partial \left(\frac{dx_n}{dt}\right)/\partial x_n = 0.$$

Nondivergence means that the stochastic process defined by (66) and Lebesgue's measure on C is stationary. Then, if we assume that two successive states of the system become uncorrelated for large enough time lags, we can apply Birkoff's first theorem (e.g. Khinchin 1949) which says that the time averages

$$\overline{E}_n^T = \frac{1}{T}\int_o^T E_n(t)dt$$

converge almost surely towards the expectations $\overline{E}_n$. These can be evaluated by volume integrations along the hypercurve C (the so-called micro-canonical ensemble) ; these integrals are easier to calculate if we approximate Lebesgue's measure by a Boltzmann distribution around C :

$$P(x_n) = \left(\frac{a+b(k_n^2+\ell_o^2)}{2\pi}\right)^{1/2} \exp\left(-\frac{1}{2}\left(a+b(k_n^2+\ell_o^2)\right) E_n\right), \qquad (69)$$

which yields

$$\overline{E}_n = \left(a + b(k_n^2+\ell_o^2)\right)^{-1}. \qquad (70)$$

For a complete discussion of such statistical equilibria, originally derived by Kraichnan (1967), the reader is refered to Sadourny (1984). What can be said roughly is that the inviscid numerical solution tends to reach an equipartition of potential enstrophy among small scale modes, and an equipartition of energy among large scale modes (figure 2, from Basdevant and Sadourny 1975).

This long-term behaviour of numerical solutions is totally unrealistic and does not improve when resolution is increased (figure 2). Asymptotically, (70) yields one-dimensional energy spectra in k^{-1}, instead of k^{-3} for physical flows : this is because potential enstrophy, being unable to reach the sub-grid

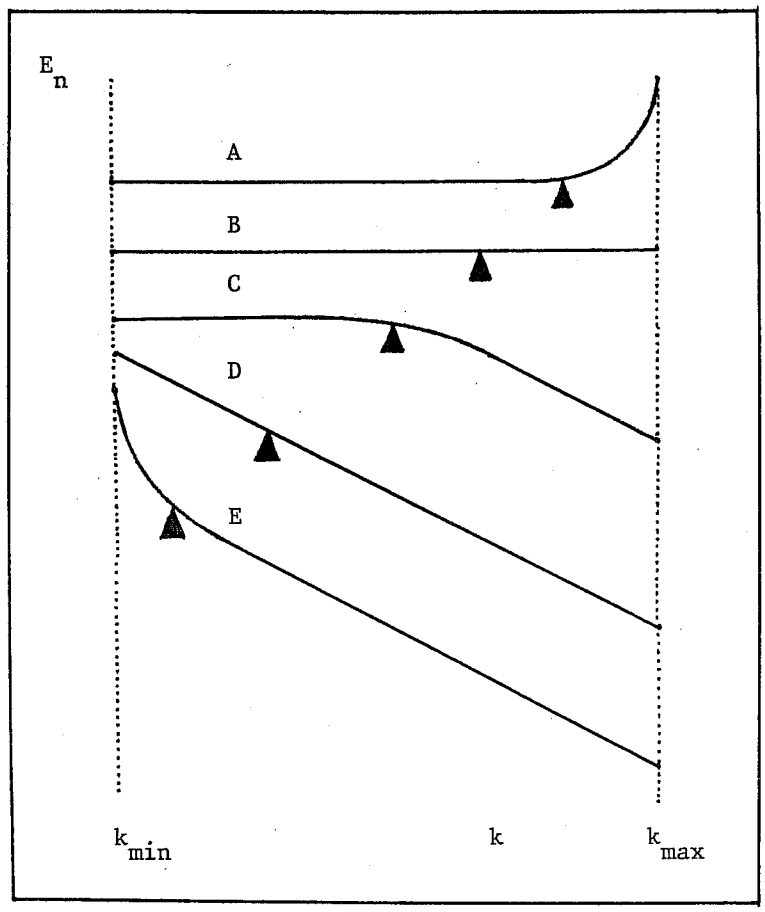

Figure 2. Equilibrium spectra for various values of $\bar{k} = (P/E)^{1/2}$, $\ell_\Theta = 0$; $\bar{k}$ is indicated by black triangles (logarithmic scales). The figure can also be seen as describing the influence of resolution, for $\bar{k}$ fixed and varying k_{max}. (Adapted from Basdevant and Sadourny, 1975).

scales, accumulates in the vicinity of the cut-off.†

3.4. Lateral diffusion : a review.

Let us assume we consider a numerical model with a cut-off wavenumber in the potential enstrophy inertial range. If we want to eliminate the trend towards artificial statistical equilibria described in §3.3., in favour of a more realistic simulation of the inertial range, we have to parameterize the potential enstrophy cascade across the cut-off wavenumber. This can be done — with variable degrees of efficiency — by a number of lateral diffusion schemes.

3.4.1. Early formulations.

The simplest formulation of lateral diffusion is the linear laplacian which mimicks molecular viscosity, but at the cut-off scale. This is of course a very crude approach ; it introduces a wide artificial dissipation range in the vicinity of the cut-off wavenumber k_c, and does not really simulate the dynamics of the inertial range. We know from §3.2 that only potential enstrophy should leave the resolved scales : energy should be strictly conserved. The linear laplacian behaves very badly in this respect, since the ratio of energy dissipated, to enstrophy dissipated is larger than k_c^{-2}. Smagorinsky (1963) introduced a nonlinear artificial viscosity, in which the viscosity coefficient, instead of being constant, is proportional to local deformation ; Leith (1968) makes it proportional to the magnitude of the local vorticity gradient. With such formulations dissipation is concentrated in regions where we expect a strong nonlinear activity ; however, the choice of a nonlinear dependency is to a large extent arbitrary. These nonlinear viscosities still dissipate energy and create artificial dissipation ranges in the vicinity of the cut-off.

3.4.2. Spectral formulations.

A more convincing approach is to try to base the formulation of lateral diffusion on a direct analysis of the sub-grid scale dynamics. Leith (1971)

† The situation is of course much worse for finite-difference models which conserve only energy. The same argument shows that in that case the solution tends, in the long run, to equipartition its energy among all modes, which corresponds to energy spectra in k^{+1}.

makes a statistical evaluation of the effect of the cut-off on nonlinear transfers, assuming a k^{-3} energy spectrum, from which he deduces a universal form for artificial viscosity $\nu(k, k_c)$. The interesting points are that $\nu(k, k_c)$ is negative for $k \ll k_c$ — a "negative viscosity" effect which ensures global energy conservation, and that it increases strongly in the close vicinity of k_c, with a cusp-like behaviour. The formulation proposed by Basdevant, Lesieur and Sadourny (1978) is more elaborate although similar in principle : in this approach, a statistical closure model of two-dimensional turbulence is actually coupled with the truncated deterministic model to actually simulate the statistical effect of the sub-grid scales. When this parameterization is translated in terms of artificial viscosity, the same properties as before : negative viscosity at large scales, cusp-like behaviour near the cut-off, are indeed observed. Both methods turn out to be extremely efficient — as one should expect — if one only looks at integral and spectral properties : energy is conserved, no artificial dissipation range appears in the energy spectrum. The situation is quite different, however, if we look at the flow in physical space ; in both cases, lateral diffusion cannot be interpreted as a local derivation operator : a disturbing consequence is that the spatial coherence of structures tend to be damaged. Another defect of these two approaches is that they are too dependent on the classical phenomenology described in §3.2. Therefore, all mechanisms which would tend to disturb this phenomenology — like, for instance, intermittency : see Basdevant, Legras and Sadourny ; Béland 1981 — will be inhibited, the classical phenomenology being imposed on the flow by the dissipation scheme.

3.4.3. Superviscosity.

"Super" viscosity is a very simple linear formulation using an interated laplacian eventually modified by a radius of deformation : $- \nu_p (\ell_o^2 - \nabla^2)^p$. Since it is linear (the coefficient ν_p is a constant), it is a fast and efficient scheme when computed in spectral space. Scale selectiveness increases with p : the dissipation range gets narrower and the ratio of energy dissipated to potential enstrophy dissipated decreases as $(k_c^2 + \ell_o^2)^{-p}$. Therefore the simulation of the inertial range gets more and more realistic as p increases ; there is a limit, however, to how large p can be for a given resolution : there seems to be an increasing function $p_c(k_c)$ such that, if $p > p_c$ for a cut-off wavenumber k_c, dissipation becomes inefficient. In other words, $p_c(k_c)$ is the optimal value of p for the cut-off wavenumber k_c ; for a resolution 128 x 128, p = 8 seems reasonable. Also, note that superviscosity, being a local operator in physical space, does not tend to destroy the spatial coherence of the flow. In fact, it may

very well be the best and fastest lateral diffusion scheme at hand.

3.4.4. The anticipated potential vorticity method (APVM)

The anticipated potential vorticity method or APVM (Sadourny and Basdevant 1981) attempts to parameterize the statistical effects of subgrid scales by returning to the very first principles of the phenomenology : potential enstrophy must be dissipated because it should cascade across the cut-off wavenumber, but energy should be exactly conserved because there is no energy flux along the potential enstrophy inertial range in the asymptotic limit. These two constraints (energy conservation, potential enstrophy dissipation) yield a diffusion operator which acts on the potential vorticity equation in the following way :

$$\frac{D\tilde{q}}{Dt} - \mathrm{div}\left(\theta\tilde{V}\,\mathfrak{P}(\tilde{V}.\mathrm{grad}\ \tilde{q})\right) = 0 \tag{71}$$

where θ is a time scale and $\mathfrak{P}$ a nondimensional positive symmetric linear operator. Since $\tilde{V}$ is non divergent (71) is equivalent to

$$\frac{\partial\tilde{q}}{\partial t} + V.\mathrm{grad}\left(q - \theta\mathfrak{P}\,(\tilde{V}.\mathrm{grad}\tilde{q})\right) = 0 \tag{72}$$

In the simplest case $\mathfrak{P} = 1$, the diffusion term appears as a simple up-wind correction, anticipating the advected field $\tilde{q}$ by a time lag θ. This choice is easiest to implement, but not very realistic ; a realistic correction must be scale dependent : most intense near the cut-off while vanishing at very large scales. We shall then define $\theta\mathfrak{P}$ by its spectral transform $\theta_n(k_n)$, a matrix of scale-selective time lags with a cusp-like behaviour in the vicinity of k_c, and $\theta_n \sim 0$ for $k_n \ll k_c$. For instance, we may use

$$\mathfrak{P} = (-\nabla^2)^p\, k_c^{-2p}. \tag{73}$$

Figure 2 (from Basdevant & Sadourny 1983) shows two energy spectra obtained from a 128 x 128 spectral barotropic model ; one with the APVM (p = 8), the other with the superviscosity method (also p = 8). There is hardly any difference except close to the cut-off : there the APVM is better in the sense that it does not produce any artificial dissipation range. This was also the case with the spectral methods of Leith(1971) and Basdevant, Lesieur & Sadourny (1978) ; but here the spectral shape has not been prescribed *a priori* : note that in figure 3 the slope is significantly steeper than -3, probably due to intermittency effects.

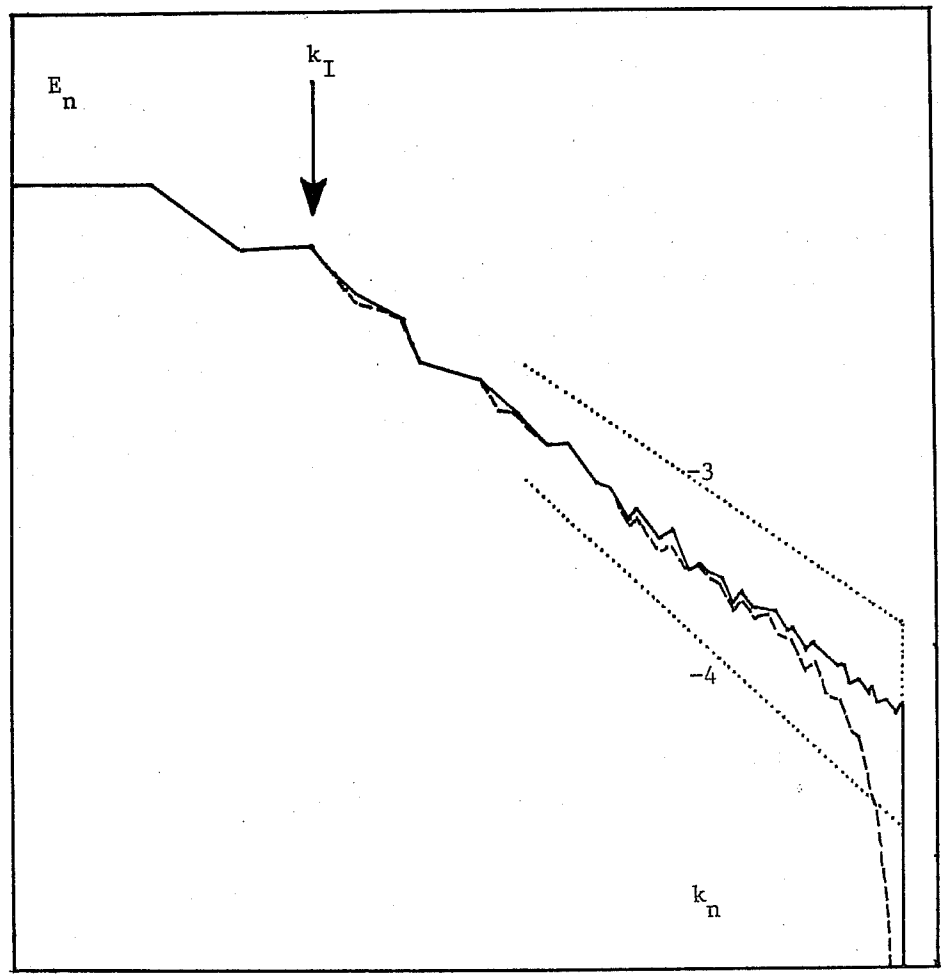

Figure 3. Comparison of energy spectra for forced barotropic turbulence, using superviscosity (discontinuous line) or APVM (continuous line). Logarithmic scales.

4. QUASI-GEOSTROPHIC TURBULENCE AND LATERAL DIFFUSION : THE BAROCLINIC CASE.

4.1. "Internal" versus "external" quasi-geostrophic turbulence.

Baroclinic quasi-geostrophic flow in its full generality is described by equations (22-23, 25-28). If one compares with barotropic flow, the main complication here is the coupling between "internal" dynamics — the advection of potential vorticity inside the fluid, described by (22-23), and "external" dynamics — the advection of geopotential or pressure perturbations along the bottom and top boundaries, described by (25-28) : our present theories of baroclinic quasi-geostrophic flow have always considered the two problems separately (Charney 1971 ; Salmon 1978, 1980 ; Blumen 1978 ; Herring 1980 ; Hoyer and Sadourny 1982 ; Sadourny and Hoyer 1982) ; the coupling problem remains open.

The "pure" internal problem is defined by setting $p' = 0$ at the top boundary and $\phi' = 0$[†] at the bottom, or :

$$\frac{\partial \Psi}{\partial s} = 0 \qquad \text{at } s = \bar{s}_T, \tag{74}$$

$$(\bar{\alpha}_s - \bar{\alpha}\frac{\partial}{\partial s})\Psi = 0 \qquad \text{at } s = \bar{s}_B, \tag{75}$$

instead of (25-28). The problem then reduces to advection of potential vorticity (22-23) between dynamically neutral boundaries (74,75).

Conversely, the "pure" external problem is formulated by setting $q' = 0$ inside the fluid domain, or

$$\left(\nabla^2 + \frac{\bar{f}}{\bar{r}}^2 \frac{\partial}{\partial s}\left(\frac{1}{\bar{\alpha}_s}\frac{\partial}{\partial s}\right)\right)\Psi = 0 \tag{76}$$

instead of (22-23). This time the problem reduces to advection of pressure and geopotential perturbations on top and bottom boundaries (25-28), the two advections being dynamically coupled through Laplace's equation (76).

For our present purpose — derivation of lateral diffusion operators consistent with quasi-geostrophic dynamics, a complete theory involving the full quasi-geostrophic set of equations (22-23, 25-28) is probably not needed.

[†]We shall from now on discard orographic effects by setting $\phi'_B(x,y) = 0$.

It is likely that an adequate formulation for lateral diffusion in the potential vorticity equation can be obtained from the sole consideration of internal dynamics, and on the other hand, an adequate formulation of lateral diffusion in the pressure and geopotential transport equations on boundaries, from consideration of external dynamics only.

In connection with this splitting of quasi-geostrophic dynamics into internal and external problems, the energy invariant (29) can be rewritten in the more convenient form

$$E = \frac{1}{2} \iint_D \left[\left(\frac{\overline{f}}{\overline{\alpha}} \psi\phi' \right)_B + (\overline{f}\psi p')_T - \int_{\overline{s}_B}^{\overline{s}_T} \overline{r}\psi q \, ds \right] dxdy, \tag{77}$$

or

$$E = -\frac{1}{2} \iint_D dxdy \int_{\overline{s}_B}^{\overline{s}_T} \overline{r}\psi q \, ds \tag{78}$$

in the internal case, and

$$E = \frac{1}{2} \iint_D dxdy \left[\left(\frac{\overline{f}}{\overline{\alpha}} \psi\phi' \right)_B + (f\psi p')_T \right] \tag{79}$$

in the external case.

A spectral formulation of the *internal* problem involves expanding ψ in terms of eigensolutions of the elliptic problem $\mathcal{D}\psi = q$, with boundary conditions (74,75) at top and bottom ; we shall admit that these eigensolutions do form a complete discrete orthonormal set :

$$\begin{aligned} \psi(x,y,s,t) &= \Sigma \, \psi_n(\underset{m}{t}) \, \Lambda_n(x,y) \, \Sigma_m(s) \, , \\ q(x,y,s,t) &= \Sigma \, q_n(\underset{m}{t}) \, \Lambda_n(x,y) \, \Sigma_m(s) \, , \end{aligned} \tag{80}$$

with

$$q_{nm} = -(k_n^2 + \ell_m^2) \, \psi_{nm} \, , \tag{81}$$

where $-\ell_m^2$ ($m = 0,1, \ldots$) are the eigenvalues of the vertical elliptic problem corresponding to eigenfunctions $\Sigma_m(s)$: $0 < \ell_o^2 < \ell_1^2 < \ldots$ We shall refer to $\Sigma_o(s)$ as to the "barotropic" mode, and to $\Sigma_n(s)$ ($n \geq 1$) as to the n-th baroclinic mode ; to ℓ_o^{-1} as to the external scale of deformation, and to ℓ_n^{-1} ($n \geq 1$) as to the n-th internal scale of deformation. Orthonormality of the set of eigenfunctions

(with respect to the mean pseudo-density $\bar{r}$) yields the spectral energy and total potential enstrophy expansions

$$E = \Sigma\, E_{nm} \quad , \quad E_{nm} = -\frac{1}{2}\,\psi_{nm} q_{nm} \ ,$$
$$P = \Sigma\, P_{nm} \quad , \quad P_{nm} = \frac{1}{2}\, q_{nm}^2 \ , \tag{82}$$

with the relation

$$P_{nm} = K_{nm}^2\, E_{nm} \ ,$$
$$K_{nm}^2 = k_n^2 + \ell_m^2 \ . \tag{83}$$

For the *external* problem, we first expand in terms of horizontal harmonics $\Lambda(x,y)$, then solve the differential equations which correspond to (76) :

$$\frac{\bar{f}^2}{\bar{r}} \frac{\partial}{\partial s} \left(\frac{1}{\bar{\alpha}_s} \frac{\partial}{\partial s}\right)\psi_n = k_n^2\, \psi_n \tag{84}$$

with boundary conditions $\psi_n(\bar{s}_T) = \psi_{Tn}$, $\psi_n(\bar{s}_B) = \psi_{Bn}$.

If we define the normalised pressure and geopotential perturbations

$$q_T = \bar{f} p'_T = \frac{\bar{f}^2}{\bar{\alpha}_s} \frac{\partial \psi}{\partial s} \qquad \text{at } s = \bar{s}_T \ ,$$
$$q_B = \frac{\bar{f}}{\bar{\alpha}}\, \phi'_B = \frac{\bar{f}^2}{\bar{\alpha}} \left(1 - \frac{\bar{\alpha}}{\bar{\alpha}_s} \frac{\partial}{\partial s}\right)\psi \qquad \text{at } s = \bar{s}_B \ , \tag{85}$$

the solution of (84) determines a positive symmetric linear application $T : (\psi_{Tn}, \psi_{Bn}) \to (q_{Tn}, q_{Bn})$, with orthonormal eigenvectors $\Delta_{no} = (\Delta_{Tno}, \Delta_{Bno})$, $\Delta_{n1} = (\Delta_{Tn1}, \Delta_{Bn1})$, and positive eigenvalues K_{no}^2, K_{n1}^2 : $0 < K_{no} < K_{n1}$. As for the internal problem, we shall refer to Δ_{no} as to the barotropic mode and to Δ_{n1} as to the baroclinic mode. We shall also define for the external problem external and internal scales of deformation, respectively ℓ_o^{-1}, ℓ_1^{-1} , with

$$\ell_o = \lim_{k_n \to o} K_{no} \ ,$$
$$\ell_1 = \lim_{k_n \to o} K_{n1} . \tag{86}$$

Total energy : E, and total available potential energy on boundaries : $P = P(\bar{s}_T) + P(\bar{s}_B)$, can be expanded as

$$E = \Sigma\,(E_{no} + E_{n1}), \qquad E_{nm} = -\frac{1}{2}\,\psi_{nm} q_{nm},$$
$$P = \Sigma\,(P_{no} + P_{n1}), \qquad P_{nm} = \frac{1}{2}\,q_{nm}^2\,, \tag{87}$$

where ψ_{nm}, q_{nm} are the spectral expansion components of (ψ_T, ψ_B), (q_T, q_B) along the Δ_{nm} basis ; E_{nm} and P_{nm} being related by

$$P_{nm} = K_{nm}^2\, E_{nm}\,, \qquad m = 0,1\,. \tag{88}$$

Note that, as soon as we choose a spectral approach, we loose track of all invariants except the *global quadratic* ones : thus we loose track, not only of the *generalised invariants* $P_A(s)$, $P_A(\bar{s}_T)$, $P_A(\bar{s}_B)$, but also, of the *detailed quadratic invariants* $P(s)$, $P(\bar{s}_T)$, $P(\bar{s}_B)$, which are not easily describable in spectral space. The fact that our phenomenology — which follows — is based on the invariance of E and P only may be seen as a rather severe restriction.

4.2. Phenomenology of fully-developed baroclinic turbulence.

We consider now a horizontally homogeneous, horizontally isotropic, internal or external quasi-geostrophic turbulence over an infinite horizontal plane. In this section therefore, wavenumbers will take continuous values and will be denoted by k instead of k_n. We assume thermal forcing at horizontal scale k_I^{-1} and vertical scale ℓ_I^{-1} (I-th baroclinic mode, with of course I = 1 for the external problem) ; we also assume a stationary energy injection rate ε, corresponding to a P-injection rate $\pi = K_I^2 \varepsilon$.

Like in the barotropic case, we shall assume that excitation propagates in the energy spectrum of the flow in such a way as to produce an ever-increasing horizontal wavenumber band (k_-, k_+) within which the flow is statistically stationary. From this assumption we shall try to establish the phenomenology of quasi-geostrophic turbulence in the fully developed limit $k_- \to 0$, $k_+ \to \infty$.

Like in section 3.2, we denote by ε_+, π_+ the spectral fluxes of E and P towards horizontal wavenumbers greater than k_+ ; and by ε_-, π_- the spectral fluxes of E and P towards horizontal wavenumbers smaller than k_-. It is easily seen that relations (49) are still valid :

$$\varepsilon_+ + \varepsilon_- = \varepsilon,$$
$$\pi_+ + \pi_- = \pi\ ; \tag{89}$$

However, in order to go further, we need to know at least the qualitative behaviour of the eigenvalues $K_m^2(k)$ — generalisation to the k-continuous case of the eigenvalues K_{nm}^2 introduced in 4.1. These are sketched on figure 4a for the internal case, and figure 4b for the external case. At low horizontal wavenumbers, the internal and external problems are roughly equivalent. In both cases the limits of $K_m(k)$ as the horizontal wavenumber approaches zero are the successive deformation wavenumbers. Furthermore, expanding the left-hand side of (84) shows that, at low horizontal wavenumbers, $\partial/\partial s$ is of the order of k^2 — which means that, in the external problem, the departure of $K_m^2(k)$ from ℓ_m^2 is of the order of k^2 like for the internal problem. At large horizontal wavenumbers on the contrary, the internal and external problems depart significantly from each other. In the external case, for fixed m, $K_m^2(k)$ is of the order of k (this again follows from (84), which yields $\partial/\partial s$ of the order of k for large k); in the internal case, it is asymptotic to k^2.

Then the equivalent of (50) :

$$\pi \geqq \pi_+ \geqq \qquad K_o^2(k_+)\ \varepsilon_+ \tag{90}$$

yields $\varepsilon_+ \to 0$, $\varepsilon_- \to \varepsilon$ in the asymptotic limit. Thus the existence of a reverse energy cascade is established for both internal and external quasi-geostrophic turbulence . The question which remains open, is how this reverse energy cascade is partitioned between the various vertical modes (this partition will in turn determine how much P is carried to infinitesimal scales). For answering this question we now need a more detailed analysis.

Like in the barotropic case the straining of a particular structure is effected by velocity gradients with horizontal and vertical scales larger than its own. The straining time scale for a structure at wavenumbers k, ℓ_m can then be estimated as

$$\tau_m(k) \sim \left(\sum_{m' \leqq m} \hat{\tau}_{m'}^{-2}(k) \right)^{-1/2}, \tag{91}$$

with

$$\hat{\tau}_m(k) \sim \left(\int_o^k \frac{p^4}{K_m^2(p)}\, E_m(p)\,dp \right)^{-1/2}, \tag{92}$$

(91,92) are a straightforward extension of (54) to the baroclinic case, $\hat{\tau}_m(k)$ refering to the time scale of the straining effected by the m-th baroclinic component alone. We can expect that in the asymptotic limit ($k \to 0$) of the reverse

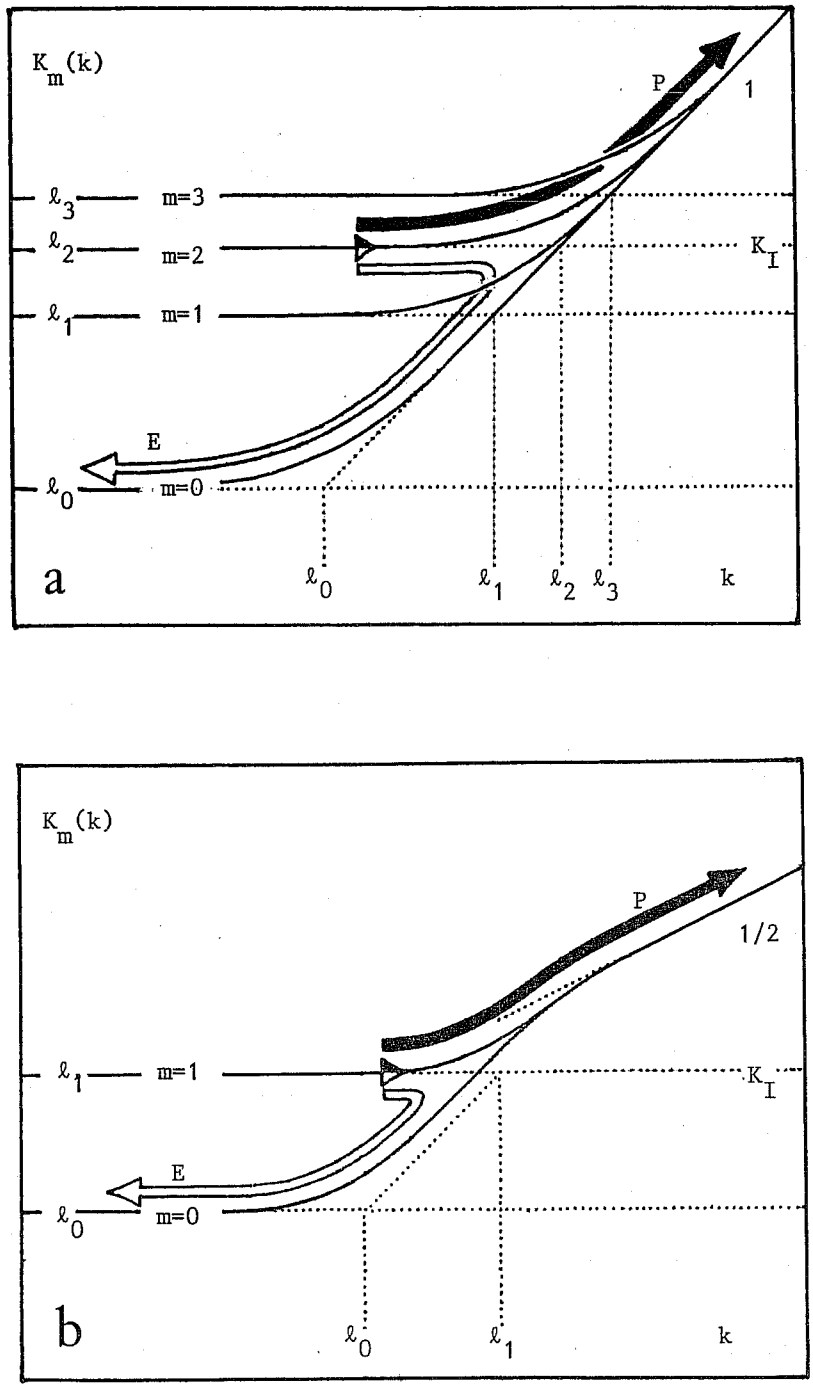

Figure 4. Disbribution of eigenvalues $K_m(k)$ in the internal case (a) and external case (b). (logarithmic scales, asymptotic slopes indicated). P-flux diagrams in black arrows, E-flux diagrams in white arrows. Black and white triangle shows thermal injection scale.

energy cascading range,

$$E_m(k) < E_{m'}(k) \qquad \text{for} \qquad m > m' \ ; \tag{93}$$

this decrease of energy with increasing vertical wavenumber is reasonable and sustained by statistical equilibrium arguments (see section 4.3). Further, in the same asymptotic limit,

$$K_m^2(p) \to \ell_m^2 > \ell_{m'}^2 \qquad \text{for} \qquad m > m'. \tag{94}$$

Then we see that, because of (93,94), $\hat{\tau}_o^{-2}(k)$ will be the dominant term in (91). In other words, the most efficient straining in the energy inertial range will be due to barotropic structures which carry the largest amount of kinetic energy.

From this it follows that all baroclinic modes ($m > 1$) are essentially passively advected by barotropic flow in the energy cascading range. Therefore, baroclinic energy will be drained, like a passive scalar, towards smaller scales. In other words, the reverse energy cascade will be concentrated in the barotropic modes : in the fully developed limit,

$$\begin{aligned} \pi_- &\to \ell_o^2 \, \varepsilon \ , & \varepsilon_- &\to \varepsilon, \\ \pi_+ &\to (K_I^2 - \ell_o^2)\varepsilon, & \varepsilon_+ &\to 0. \end{aligned} \tag{95}$$

This double cascade scheme is illustrated on figures 4a, 4b. Note that in K-space, the situation is exactly reminiscent of the barotropic case, energy flowing from K_I to the lowest K, while P mostly flows from K_I to infinite K. Also note that the P-cascade towards infinitely small horizontal scales will be eventually carried by all vertical modes, since the m first baroclinic modes are in practice undistinguishible from the barotropic mode as soon as k gets larger than ℓ_m.

The last point in phenomenology concerns the derivation of spectral laws for energy distribution. Here we proceed like in section 3.3. Looking first at the larger scales in the reverse energy cascading range, we may recall our earlier remark that the internal and external problems are roughly equivalent there ; also, the reverse cascade is confined within barotropic modes. Then, all the results of section 3.2 hold and the barotropic energy distribution follows (60,61) since thermal injection ensures $\ell_o < K_I$:

$$E_o(k) \sim C_- \, \varepsilon^{2/3} \, k^{-5/3} \qquad (\ell_o < k < K_I) \tag{96}$$

$$E_o(k) \sim 2^{1/3} C_- \, \varepsilon^{2/3} \, \ell_o^{2/3} \, k^{-7/3} \qquad (k < \ell_o) \tag{97}$$

In the P-inertial range, we do not need to separate the different vertical modes. (91,92) are equivalent to

$$\tau(k) \sim \left[\int_o^k P^2 E(p)dp\right]^{-1/2} \qquad (98)$$

in the internal case, where $K_m^2(k) \sim k^2$, and to

$$\tau(k) \sim \left[\int_o^k P^3 E(p)dp\right]^{-1/2} \qquad (99)$$

in the external case, where $K_m^2(k) \sim k$. Here

$$E(k) = \sum_m E_m(k).$$

On the other hand, the P-cascade rates are estimated as

$$\pi_+ = k^3 E(k)/\tau(k) \qquad (100)$$

in the internal case, and

$$\pi_+ = k^2 E(k)/\tau(k) \qquad (101)$$

in the external case. (98,100) yield

$$E(k) \sim C_+ \left((K_I^2 - \ell_o^2)\varepsilon\right)^{2/3} k^{-3} \left(\mathrm{Ln}\,\frac{k}{K_I}\right)^{-1/3} ; \qquad (102)$$

thus the P-inertial range of internal quasi-geostrophic turbulence behaves exactly like the P-inertial range of barotropic turbulence. In the internal case the situation is different ; (99,101) yield

$$E(k) \sim C_+ \left((K_I^2 - \ell_o^2)\varepsilon\right)^{2/3} k^{-8/3} . \qquad (103)$$

Note that, since $P(k) \sim k\,E(k)$ at large wavenumbers, the P-spectrum which correspond to (103) obeys a -5/3 power law : this is only natural, since we may remember that P in the external case is indeed an *energy* (available potential energy on boundaries) which cascades towards infinitesimal scales ; thus (103) corresponds to an energy-inertial range spectrum.

4.3. Remarks on baroclinic instability.

We have now a general picture of (internal and external) quasigeostrophic dynamics which can be summarised as follows. When thermal energy is injected in the m_I-th baroclinic mode, it cascades back in K-space until it reaches values of K smaller than the first deformation wavenumber ℓ_1 ; afterwards the reverse energy cascade is concentrated in the barotropic modes and propagates along ever increasing horizontal scales. Simultaneously, a portion $\ell_o^2\varepsilon$ of the potential enstrophy (or available potential energy on boundaries in the external case) also cascades back to barotropic large scales ; the remaining part$(K_I^2-\ell_o^2)\varepsilon$ cascades down to infinitesimal scales.

This general picture requires that thermal (in other words, potential) energy is converted into kinetic energy in the horizontal-wavenumber band (ℓ_o, K_I) : this is the well known process of baroclinic instability, which keeps feeding the barotropic large scales. The phenomenology derived in 4.2 demonstrates its existence, and describes its generating mechanism as the combined effect of energy trapping at large K's, and the draining of P towards small K's.

4.4. Truncated inviscid model flows : statistical equilibria.

As in the barotropic case (section 3.3), truncation blocks the cascade processes at the cut off wavenumbers. Discrete models which formally conserve E and P evolve towards statistical equilibria

$$E_{nm} = (a+bK_{nm}^2)^{-1} \qquad (104)$$

in absence of dissipation and forcing. (104) is formally identical to (70) and is derived in exactly the same way, provided we admit (like in 4.2) that the *detailed* conservations of P(s), $P(\bar{s}_T)$, $P(\bar{s}_B)$ do not play a significant dynamic role compared to the *global* conservation of P. Also, note that (104) indeed shows that the quasi-geostrophic nonlinear dynamics tend to accumulate energy in the smallest K's, an assumption already used in the phenomenology of (4.2).

The trend of truncated inviscid model flows towards statistical equilibria reflects a realistic tendency of nonlinear dynamics to propagate E towards smaller K's and P towards larger K's. The final distribution, however, is strongly biased by the truncation effect, which replaces inertial range spectra by equipartition spectra.

Numerical models therefore need lateral diffusion operators designed to simulate accurately the cascade processes across the artificial upper cut-off wavenumber k_c.

4.5. Lateral diffusion, or the parameterisation of baroclinic instability in low-resolution models.

We consider now numerical models of quasi-geostrophic flow thermally forced at the generalised wavenumber K_I. We have seen in 4.2 that all the thermal energy injected, after being converted into kinetic energy by baroclinic instability processes, eventually shows up in barotropic large scales : therefore, we must require that lateral diffusion operators strictly conserve the total energy E ; but we must also require that they dissipate the proper amount of the invariant P, in order to ensure appropriate conversions of potential energy into kinetic energy. These two requirements will be the main guidelines for proper parameterisation of sub-grid scale baroclinic instability in numerical models.

The problem is easiest to solve for high resolution models. By high resolution model we mean a model whose cut-off wavenumber is significantly larger than the generalised thermal forcing wavenumber : $k_c \gg K_I$. Then, from section 4.2 (see figure 4), we know that baroclinic instability will naturally keep the energy away from the cut-off scale : in that case, any diffusion operator like, for example, super-viscosity, will essentially dissipate P and not E. In other words, this is the case where resolution is high enough to resolve the main processes of baroclinic instability.

Now, for low-resolution models ($k_c \lesssim K_I$), truncation occurs within the natural baroclinic instability wavenumber band (ℓ_1, K_I), or, in other words, within the natural path of the energy cascade (figure 4). In that case the parameterisation of baroclinic instability becomes a crucial problem which determines the design of diffusion operators.

As an example of ordinary diffusion operators, let us look at the behaviour of super-viscosity in the low-resolution case. The governing equation for $q(s)$, q_T, q_B reads

$$\frac{Dq}{Dt} + \nu_p \, (-\nabla^2)^p \, q = 0 \qquad (105)$$

if super-viscosity is defined in terms of the horizontal laplacian ; or

$$\frac{Dq}{Dt} + \nu_p (-\mathbb{D})^p \, q = 0 \qquad (106)$$

for the internal case, if we define super-viscosity in terms of the three-dimensional laplacian $\mathfrak{D}$, and

$$\frac{Dq}{Dt} + \nu_p T^p q = 0 \qquad (107)$$

for the external problem (see section 4.1 for the definition of T). The two formulations (105), (106-107) may look different at first sight, but are indeed equivalent in the vicinity of $k_c \sim K_I$, where dissipation is concentrated. On (106-107) we see that the ratio of E-dissipation to P-dissipation is, in the super-viscosity case, of the order of K_I^{-2} :

$$\frac{\delta E}{\delta P} \sim K_I^{-2} \qquad (108)$$

Assuming that δP is "tuned" to the right order of magnitude (95), we get

$$\delta E \sim (1 - \ell_o^2/K_I^2)\ \varepsilon. \qquad (109)$$

Thus superviscosity induces, in the low-resolution case ($k_c \sim K_I$), an energy dissipation of the order of energy injection. This means a very low efficiency of the numerical model in simulating the large scale barotropic modes ; the reverse energy cascade which normally feeds these modes is significantly hindered by dissipation.

The Anticipated q - method (AqM) is a generalisation of the Anticipated Potential Vorticity method to the (internal, external, or coupled) baroclinic case. The generic equation reads

$$\frac{Dq}{Dt} - \underline{V}.\ \mathrm{grad}\left(\theta\ \mathfrak{P}\ (\underline{V}.\ \mathrm{grad}q)\right) = 0, \qquad (110)$$

applied to q(s), q_T, q_B. Here energy is exactly conserved and P(s), $P(\overline{s}_T)$, $P(\overline{s}_B)$ are dissipated : the reverse energy cascade remains realistic in spite of low-order truncation, which means proper conversions of potential energy into kinetic energy. The AqM appears therefore as an efficient dynamical parameterisation of subgrid scale baroclinic instability. It has been tested by Sadourny and Basdevant (1984) on thermally forced two-level baroclinic flow, with $\ell_1 = K_I = 15$.

Figure 5 shows the energy spectra for three test-cases : (a) high resolution ($\ell_1 = K_I \ll k_c = 61$) control case ; (b) low-resolution ($\ell_1 = K_I = k_c = 15$) with superviscosity (p = 8) ; (c) low-resolution ($\ell_1 = K_I = k_c = 15$) with AqM ($\mathfrak{P}$ given by (73), p = 8). The AqM parameterisation appears to be quite efficient

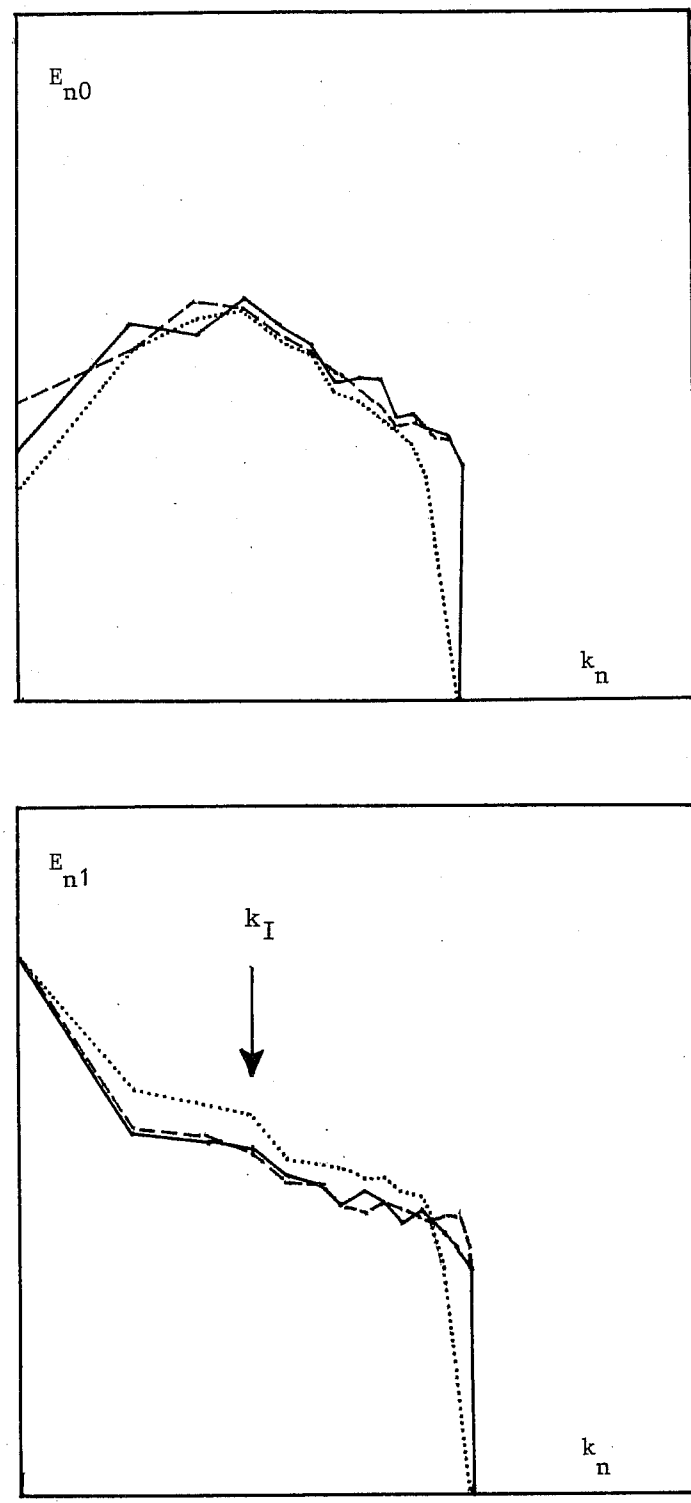

Figure 5. Barotropic (E_{n0}) and baroclinic (E_{n1}) energy spectra of two-layer internal quasi-geostrophic turbulence thermally forced at $k_I = 4$ (vertical arrow). Continuous line : control experiment ($k_{max} = 61$) truncated for display at $k_{max} = K_I = 15$). Dotted line : super-viscosity, low resolution ($k_{max} = K_I = 15$). Discontinuous line : AqM, same low resolution.

in simulating the expected level of excitation in both barotropic and baroclinic modes, in spite of severe truncation. This means that the proper amount of thermal energy is actually converted into kinetic energy by the diffusion operator, and cascaded back into larger scales. Superviscosity, on the other hand, is significantly less efficient : it underestimates barotropic energy, and overestimates baroclinic energy ; thus, in the super-viscosity case, only a part of the thermal energy injected is actually converted into kinetic energy — another part is spuriously dissipated, while a third part artificially remains in the baroclinic modes, in accordance with the phenomenological theory of Sadourny and Hoyer (1982).

The AqM seems therefore a very promising approach for designing dynamically efficient, low-order models. Its extension to the primitive equation case is straightforward, provided the equations are written in entropy coordinate form. (110) can be directly applied to Ertel's potential vorticity equation, and to the transport equations of s_T and s_B ; it can also be translated into momemtum form :

$$\frac{D\underline{V}}{Dt} + (f - \theta \underset{\sim}{\mathfrak{P}} \underline{V} \cdot \mathrm{grad}\eta)\mathrm{N}\times\mathrm{V} + \mathrm{gradS} = 0, \qquad (111)$$

for the inside flow.

5. REFERENCES

Arakawa, A., 1966 : Computational design for long-term numerical integration of the equations of fluid motion = two-dimensional incompressible flow. J. Comp. Phys. 1, 119.

Arakawa, A., 1984 : in same volume.

Basdevant, C. and R. Sadourny, 1975 : Ergodic properties of inviscid truncated models of two-dimensional incompressible flows. J. Fluid Mech., 69, 673.

Basdevant, C., M. Lesieur and R. Sadourny, 1978 : Sub-grid scale modeling of enstrophy transfer in two-dimensional turbulence. J. Atmos. Sci., 35, 1028.

Basdevant, C., B. Legras and R. Sadourny ; M. Béland, 1981 : A study of barotropic model flows : intermittency, waves and predictability. J. Atmos. Sci., 38, 2305.

Blumen, W., 1978 : Uniform potential vorticity flows : Part I. Theory of wave interactions and two-dimensional turbulence. J. Atmos. Sci., 35, 774.

Charney, J.G., 1971 : Quasi-geostrophic turbulence. J. Atmos. Sci., 28, 1087.

Charney, J.G., and G.R. Flierl, 1981 : in : Evolution of Physical Oceanography, M.I.T. Press, 504.

Herring, J.R., 1980 : Statistical theory of quasi-geostrophic turbulence. J. Atmos. Sci., 37, 969.

Hoyer, J.-M. and R. Sadourny, 1982 : Closure modeling of fully-developed baroclinic instability. J. Atmos. Sci., 39, 707.

Kato, T., 1967 : On the classical solution of the two-dimensional non stationary Euler equation. Arch. Ration. Mech. Anal., 25, 303.

Khinchin, A.I., 1949 : Mathematical foundations of information theory. Dover.

Kraichnan, R.H., 1967 : Inertial ranges in two-dimensional turbulence. Phys. Fluids, 10, 1417.

Kraichnan, R.H., 1971 : Inertial ranges in two- and three-dimensional turbulence. J. Fluid Mech., 47, 525.

Leith, C.E., 1968 : Diffusion approximation for two-dimensional turbulence. Phys. Fluids, 11, 671.

Leith, C.E., 1971 : Atmospheric predictability and two-dimensional turbulence. J. Atmos. Sci., 28, 145.

Sadourny, R., 1984 : Quasi-geostrophic turbulence : an introduction. In : Turbulence and Predictability in Geophysical Fluid Dynamics and in Climate Dynamics. Società Italiana di Fisica, in press.

Sadourny, R., and C. Basdevant, 1981 : Une classe d'opérateurs adaptés à la modélisation de la diffusion turbulente en dimension deux. C.R. Acad. Sci. Paris, 292, II, 1061.

Sadourny, R., and C. Basdevant 1984 : Parameterisation of barotropic-baroclinic instability in low-resolution quasi-geostrophic models. In preparation.

Salmon, R., 1978 : Two-layer quasi-geostrophic turbulence in a simple special case. Geophys. Astrophys. Fluid Dyn. 10, 25.

Salmon, R., 1980 : Baroclinic instability and geostrophic turbulence. Geophys. Astrophys. Fluid Dyn. 15, 167.

Smagorinsky, J., 1963 : General circulation experiments with the primitive equations. I. The basic experiment. Mon. Wea. Rev., 91, 164.